

## **Electronic Supplementary Information**

### **Single Gold Bipyramids with Sharp Tips as Sensitive Single Particle Orientation Sensors in Biological Studies**

So Young Lee<sup>1</sup>, Yeji Han<sup>1</sup>, Jong Wook Hong<sup>1</sup>, and Ji Won Ha<sup>1\*</sup>

<sup>1</sup>Department of Chemistry, University of Ulsan, 93 Daehak-Ro, Nam-Gu, Ulsan 44610, South  
Korea

\*To whom correspondence should be addressed.

**J. W. Ha**

Phone: +82-52-259-2347

Fax: +82-52-259-2348

E-mail: [jwha77@ulsan.ac.kr](mailto:jwha77@ulsan.ac.kr)

This document contains experimental methods, supplementary figures (Figure S1 to S14), and a  
supplementary movie (Movie S1).

## **MOVIE**

**Movie S1:** Rotational dynamics of transferrin-modified AuBPs on a live cell membrane at a temporal resolution of 50 ms under DIC microscopy. The AuBPs were measured at 700 nm close to their longitudinal SPR wavelength. Flickering DIC images are observed in the movie during the dynamic process.

## Experimental Methods

**1) Orientation-dependent DIC Images of Single Au Bipyramids.** In DIC microscopy the incident beam is split into two orthogonally polarized beams in the two bright and dark polarization directions by the first Nomarski prism (Fig. S9). These two beams are separated by a certain distance (usually a few hundred nanometers) along the shear direction. When two beams pass through the specimen, they generate image contrasts for optical path length gradients in the specimen. Therefore, each of the two orthogonally polarized beams generates an independent intermediate image. One such image is shifted laterally by  $\sim 100$  nm and then overlapped with the other to generate the final interference image. For anisotropic shape of AuBPs, the two intermediate images are different because the two illumination beams are phase-delayed to different extents, depending on the orientation of the AuBP relative to the two polarization directions. Therefore, the DIC images of AuBPs appear as diffraction-limited spots with disproportionate bright and dark parts and they show different bright and dark intensities depending on the AuBP orientation. For example, the darkest (or brightest) intensity is observed when the longitudinal axis of a AuBP is parallel to the dark (or bright) polarization axis. The bright and dark intensities are changed periodically as a function of the orientation angle  $\varphi$  and the intensities from bright and dark polarization directions are anti-correlated for single AuBPs.

**2) Determining the Orientation Angle of Single Au Bipyramids.** In DIC microscopy we can estimate the orientation of AuBPs from their focused DIC image patterns. There are two methods to determine the orientation angle of single AuBPs in the focal plane. First, the DIC

image patterns of a AuBP are periodically changed as a function of orientation angle. Therefore, we can simply estimate the orientation angle of AuBPs from their characteristic orientation-dependent DIC image patterns. For example, the totally bright intensity suggests that the orientation angle of a AuBP is close to  $90^\circ$ , meaning the long axis of a AuBP is parallel to the bright polarization direction. Second, the DIC polarization anisotropy based on the intensity analysis can also enable us to determine the spatial orientation of single AuBPs.

**3) Calculation of the orientation angle  $\varphi$  from the DIC polarization anisotropy  $P$ .** Two orthogonal intensities from bright and dark polarization directions are obtained in DIC microscopy. The DIC bright intensity of a AuBP is proportional to the fourth power of the sine of the orientation angle  $\varphi$  between the long axis of a AuBP and the dark axis. In addition, the DIC dark intensity is proportional to the fourth power of the cosine of the orientation angle  $\varphi$ . Therefore, the normalized bright and dark intensities ( $I_{B,N}$ ,  $I_{D,N}$ ) as a function of the orientation angle  $\varphi$  can be written as

$$I_{B,N}(\varphi) = \sin^4(\varphi)$$

$$I_{D,N}(\varphi) = \cos^4(\varphi)$$

DIC polarization anisotropy  $P$  is defined as

$$P = \frac{I_{B,N} - I_{D,N}}{I_{B,N} + I_{D,N}}$$

Therefore, the polarization anisotropy  $P$  can be rewritten as

$$P = \frac{\sin^4(\varphi) - \cos^4(\varphi)}{\sin^4(\varphi) + \cos^4(\varphi)}$$

The orientation angle  $\varphi$  can be expressed in terms of  $P$  and the following relationship for the orientation angle  $\varphi$  as a function of  $P$  is finally obtained.

$$\varphi = \arccos \left( \sqrt{\frac{A - \sqrt{A^2 - 2A}}{2}} \right), P < 0$$

$$\varphi = \arccos \left( \sqrt{\frac{A + \sqrt{A^2 - 2A}}{2}} \right), P > 0$$

where  $A$  is defined as  $(P-1)/P$ .

**4) Simulation of Scattering Image Patterns of Au Bipyramids.** We used the simulation program developed by Enderlein and Böhmer.<sup>1</sup> The program is designed to calculate the characteristic intensity distribution from an emitter with three perpendicular emission dipoles of different emission strength. It has been widely used to determine the spatial orientation of single dye molecules.<sup>1,2</sup> The simulation program is a special Matlab based utility with a graphics user interface (GUI) for easy calculation. This program allows us to calculate exactly the defocused (or focused) images of single molecules. For using the GUI, one should download the files from the website (<http://www.joerg-enderlein.de/imagingOfSingleMolecules.html>).

The parameters that can be input are: the numerical aperture of the objective lens, magnification of imaging, extent of defocusing (or defocusing distance in micrometers),  $\kappa$  and  $R$ . For defining the emission strength ratios of the three independent dipoles, we input the parameter  $\kappa$  and  $R$  into the program. The ratio  $\kappa$  defines the ratio of the emission strength of the b- to the c-dipole (transverse dipoles) as shown below.

$$I_b / I_c = (1 - \kappa) / (1 + \kappa)$$

In this study the emission strength of the b-dipole is assumed to be same as that of the c-dipole. In addition, the ratio  $R$  defines the emission strength of the a-dipole (or longitudinal dipole) to the combined b and c dipoles (or transverse dipoles) as shown below.

$$R \times I_a + (1 - R) \times (I_b + I_c)$$

When  $R$  is 1, we only have the contribution from a-dipole (longitudinal dipole) to the image patterns. However, the other two transverse dipoles (b and c) start to contribute to the image patterns with decreasing the ratio  $R$ . That is, lower  $R$  values indicate more contributions from the two transverse dipoles. Therefore, we were able to calculate the scattering patterns of a AuBP by adjusting the important parameters.

## References

1. Böhmer, M.; Enderlein, J. *J. Opt. Soc. Am. B* **2003**, 20(3), 554-559.
2. Lieb, M. A.; Zavislan, J. M.; Novotny, L. *J. Opt. Soc. Am. B* **2004**, 21(6), 1210-1215.

## Supplementary Figures

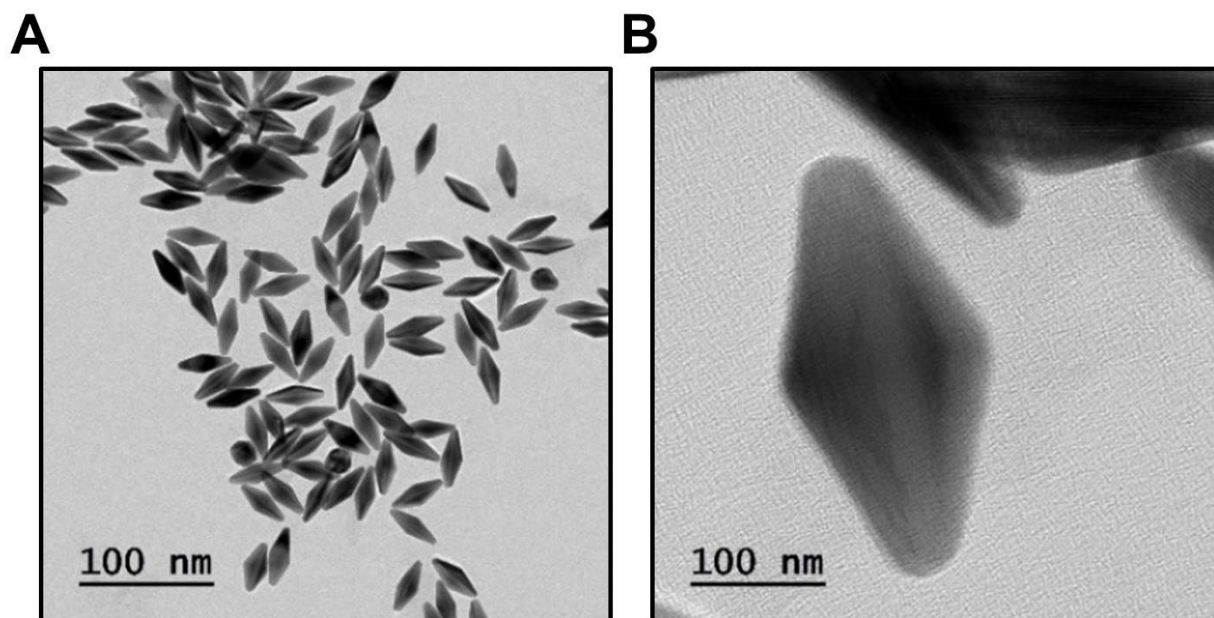


**Fig. S1** (A) TEM image of AuBPs used in this study. The average length and width are 76 nm and 26 nm, respectively. (B) Enlarged TEM image of single AuBP.

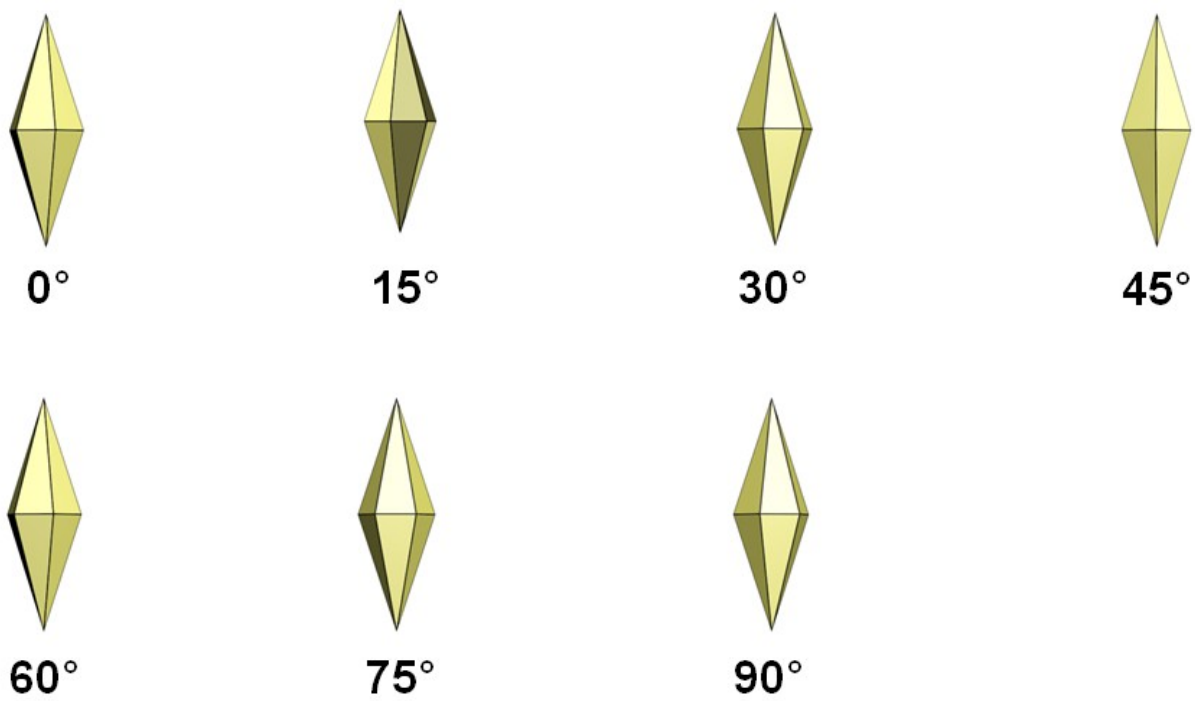


**Fig. 2** 3D structure illustration of a AuBP.



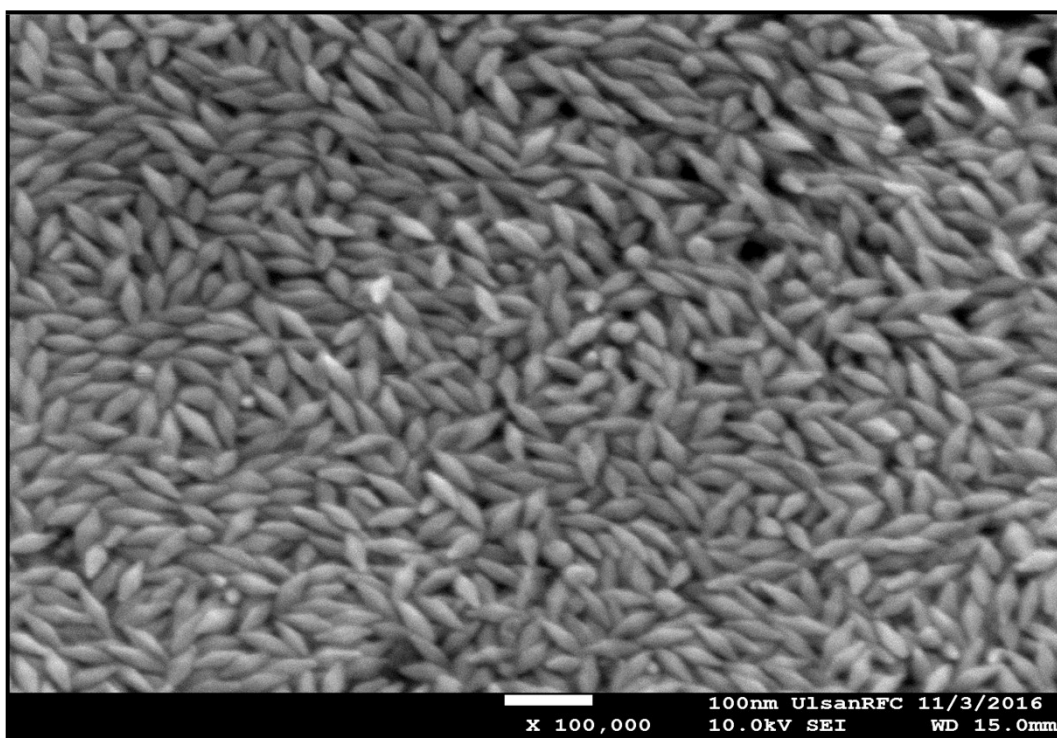


**Fig. S3** SEM image of many AuBPs that are monodisperse in size and shape.

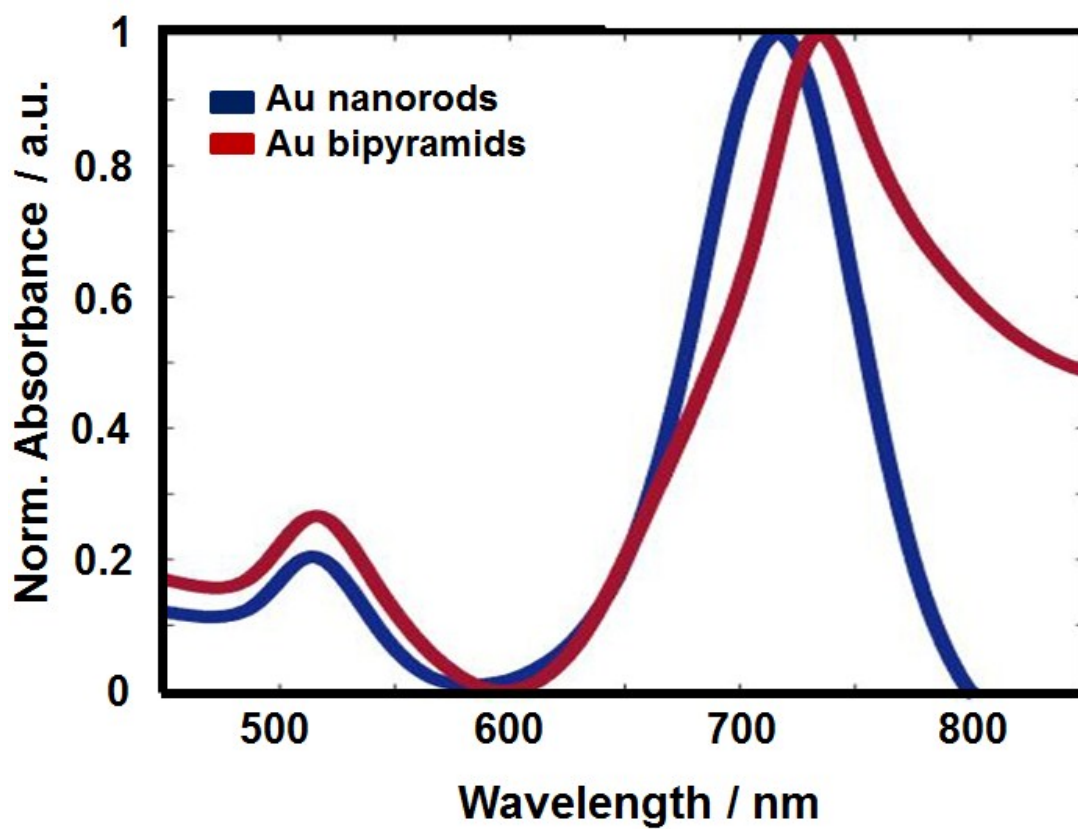


**Fig. S4** Normalized absorbance spectra of AuBPs (red-curve) and AuNRs (blue-curve) dispersed in water.

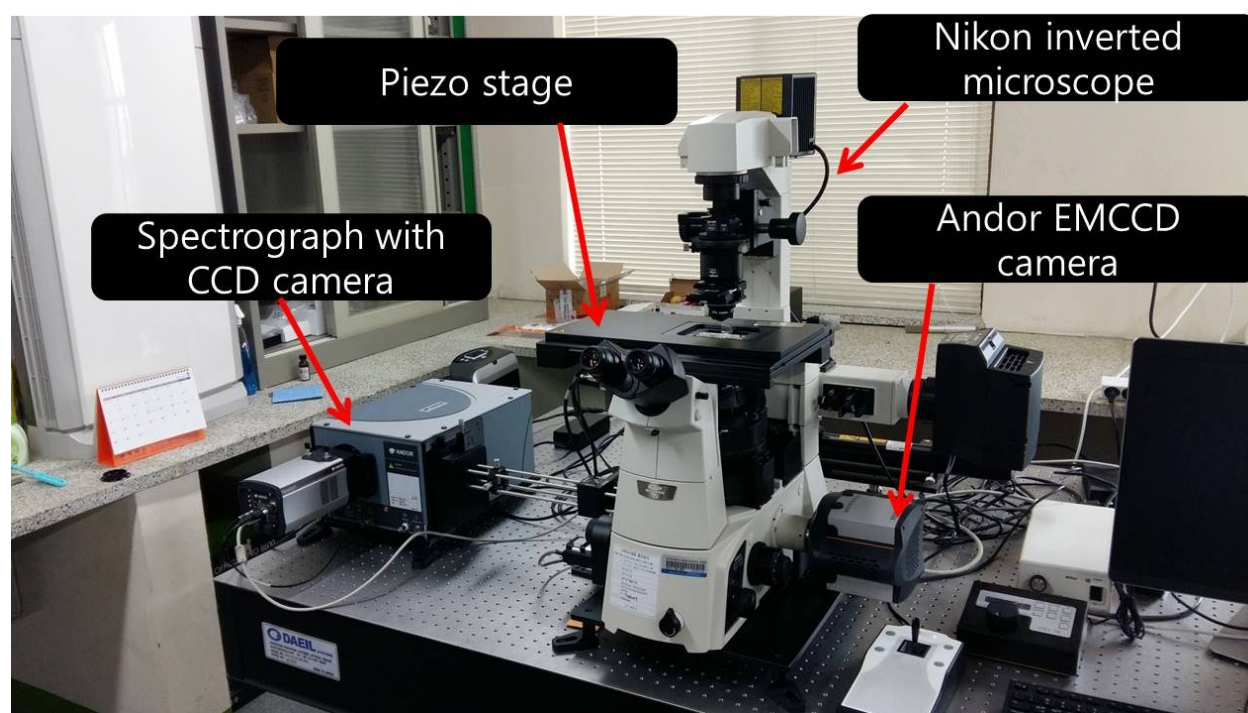


**Fig. S5** Photograph to show experimental setup for single particle microscopy and spectroscopy.

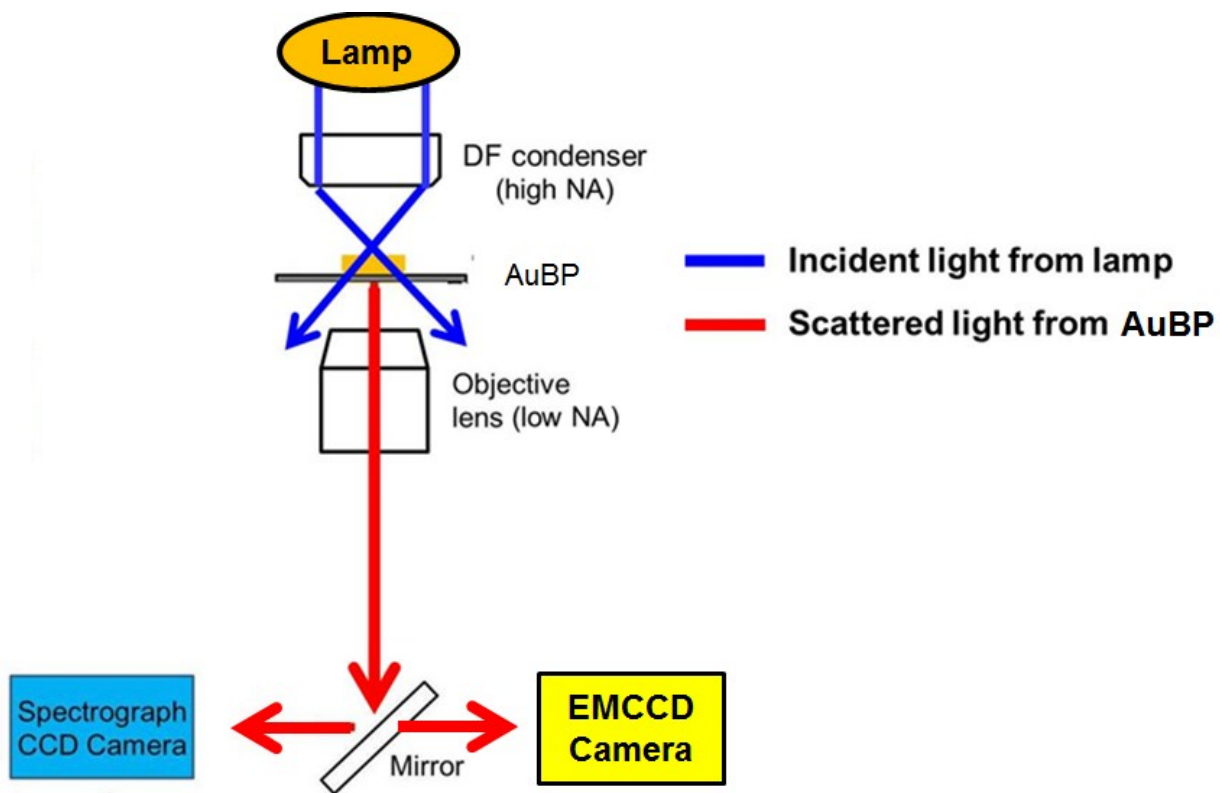


**Fig. S6** Dark-field (DF) microscopy and spectroscopy.

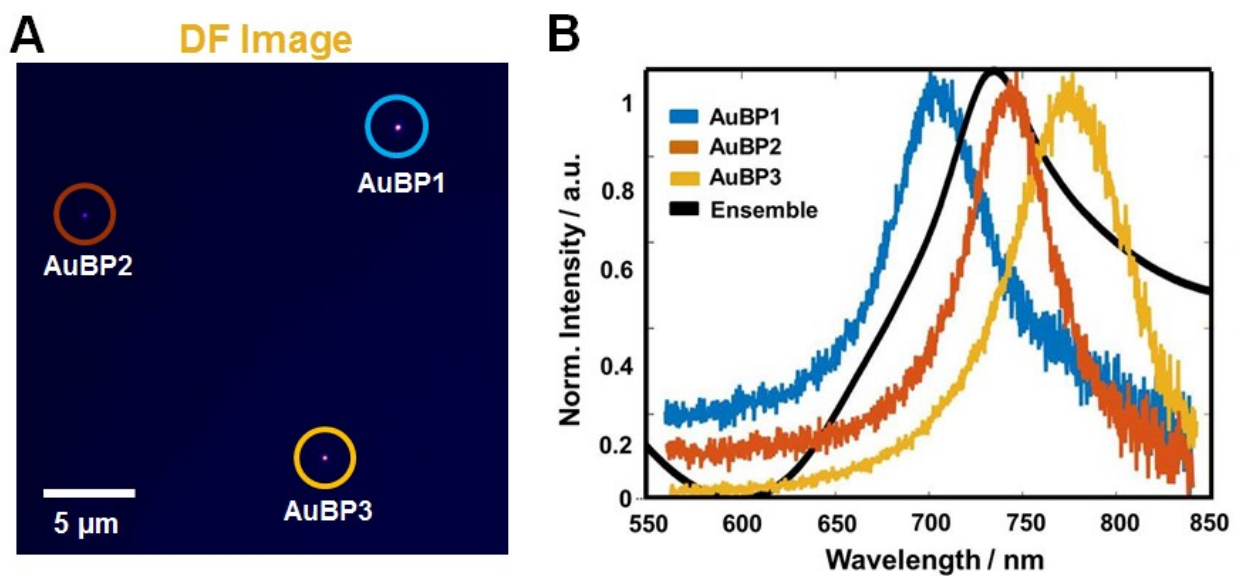


**Fig. S7** (A) DF scattering image of single AuBPs in Fig. 2. (B) Single particle scattering spectra of the three AuBPs in (A). The ensemble spectrum of AuBPs is overlaid for comparison.

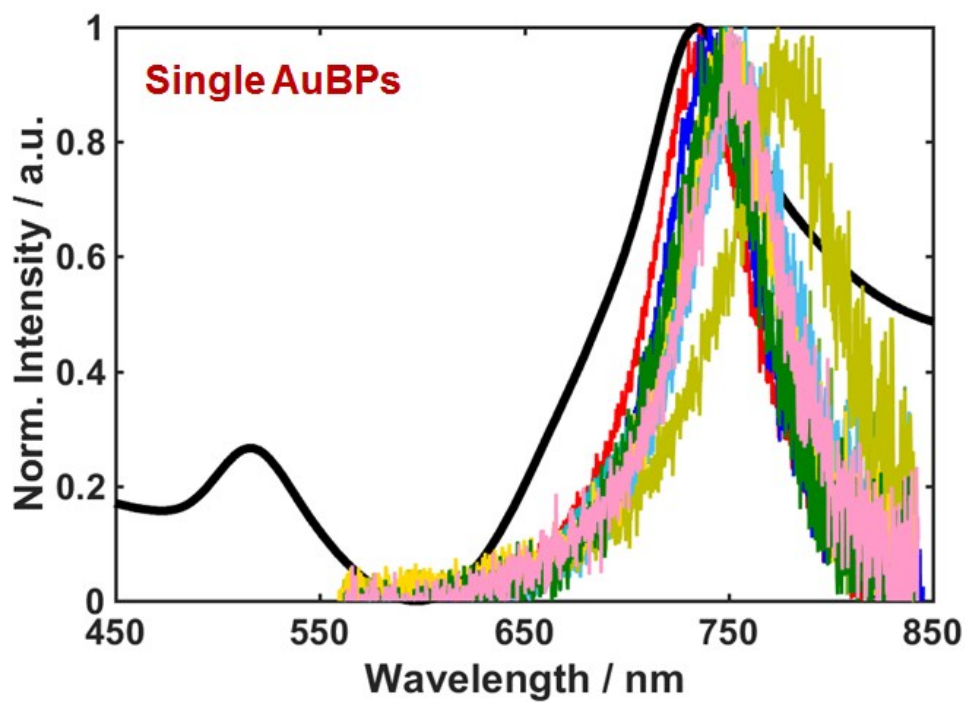


**Fig. S8** Single particle scattering spectra of AuBPs. The ensemble spectrum of AuBPs is overlaid for comparison.

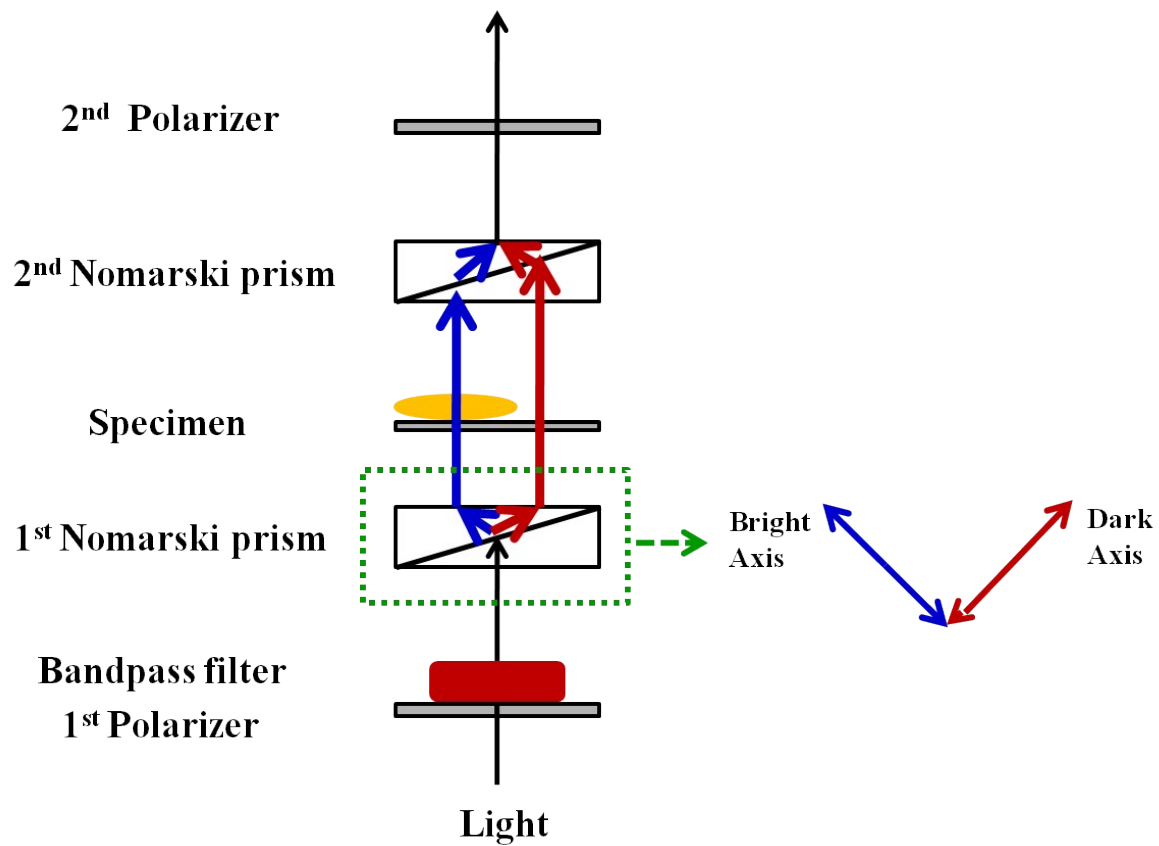


**Fig. S9** The working principle of DIC microscopy.

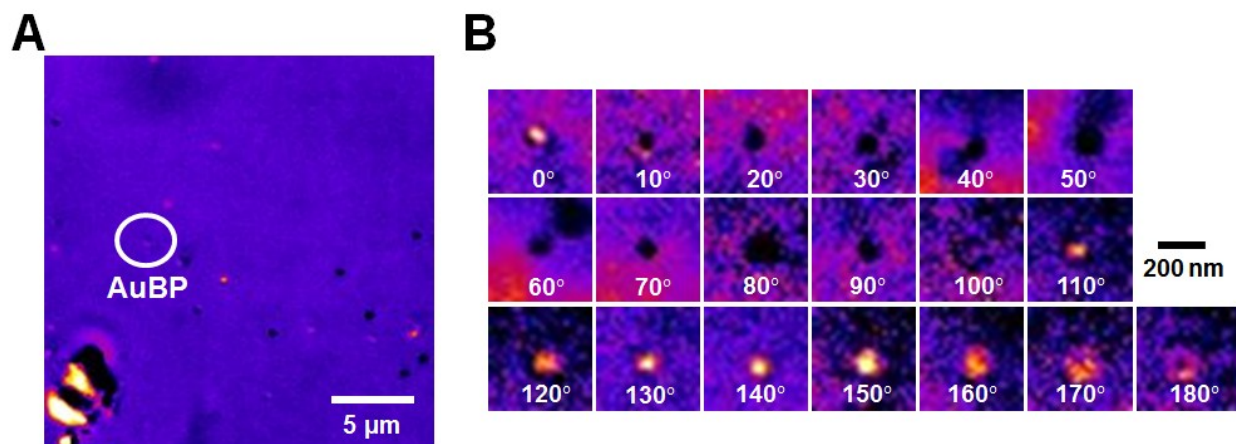


**Fig. S10** (A) DIC image of single AuBPs with different orientations on a glass slide. The AuBPs were illuminated at 700 nm. (B) Polarization-dependent DIC images of single AuBP highlighted in (A), obtained by rotating a rotational stage in increments of 10°.



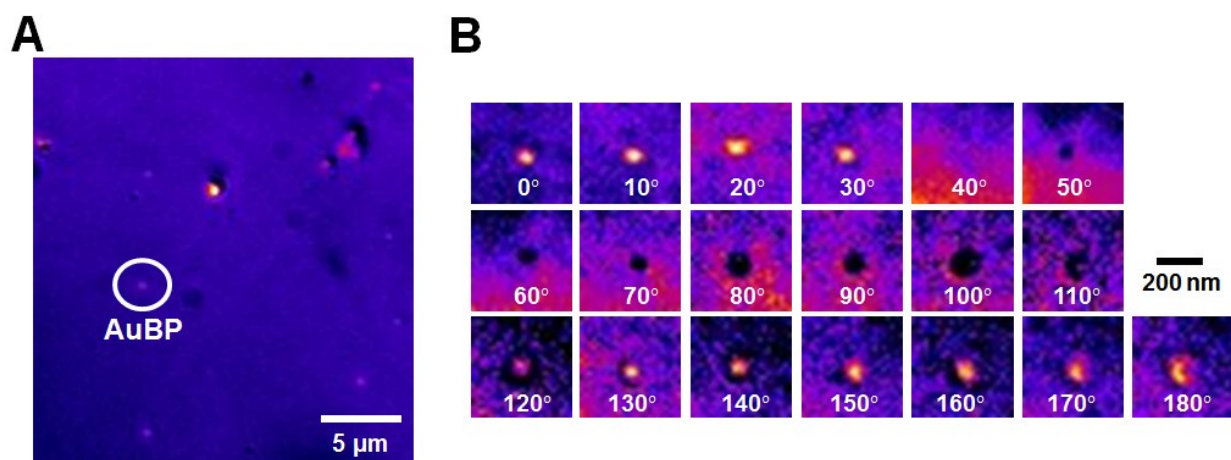


**Fig. S11** (A) DIC image of single AuBPs with different orientations on a glass slide. The AuBPs were illuminated at 700 nm. (B) Polarization-dependent DIC images of single AuBP highlighted in (A), obtained by rotating a rotational stage in increments of 10°.

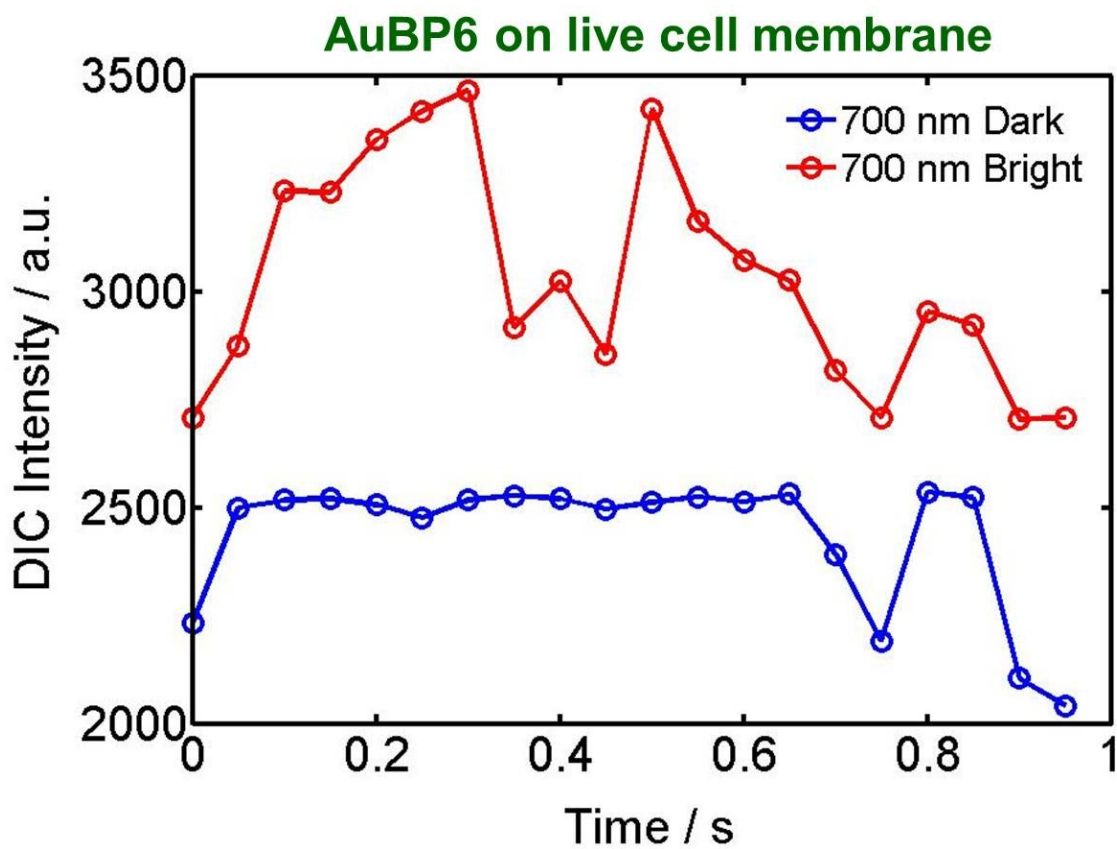


**Fig. S12** Change in the DIC intensities of AuBP6 rotating on a live cell membrane as a function of time. The AuBP6 was measured at 700 nm close to its longitudinal SPR wavelength.

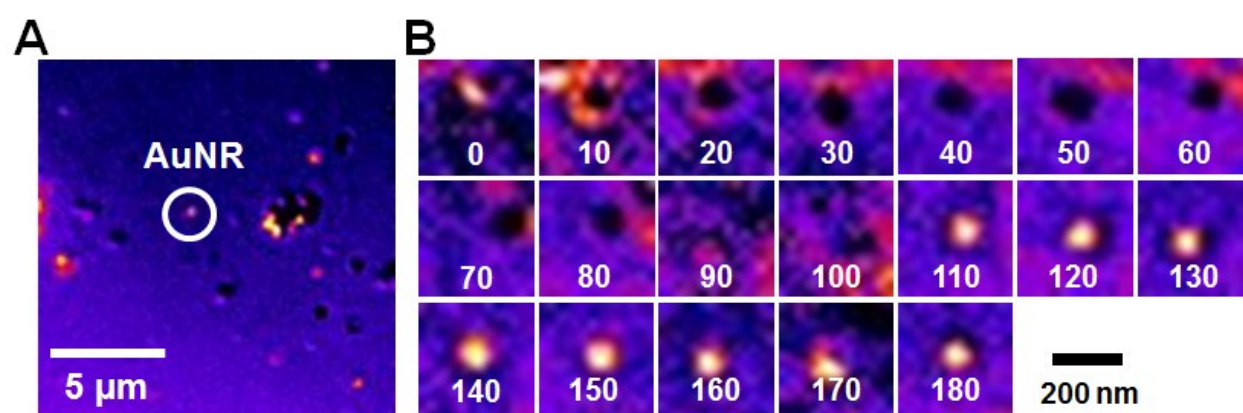


**Fig. S13** (A) DIC image of AuNRs with an average size of 25 nm × 73 nm. (B) Polarization-dependent DIC images of single AuNR obtained by rotating a rotational stage in increments of 10° at 700-nm excitation.

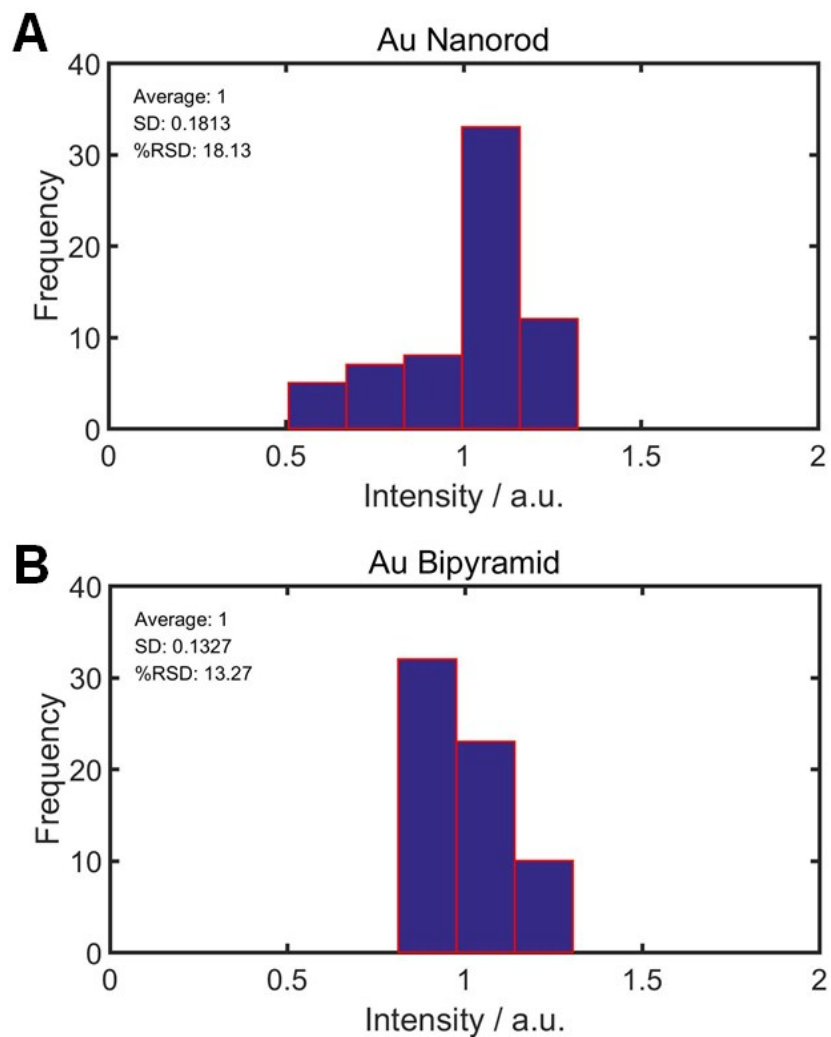


**Fig. S14** (A) The standardized histogram of the DF scattering intensity of AuNRs. (B) The standardized histogram of the DF scattering intensity of AuBPs measured under the same experimental conditions.